ISOMAse
International Society of Ocean, Mechanical and Aerospace Scientists and Engineers

Journal of Subsea and Offshore
-Science and Engineering-
30th December 2018. Vol.16 No.1

December 30, 2018

Numerical Analysis of Multi Buoy Mooring Configuration Selection

Erdina Arianti,[a,*]

[a)]*Indonesian Hydrodynamic Laboratory (IHL), Agency for The Assessment an Aplication of Technology (BPPT), Indonesia*

*Corresponding author: erdinarianti@gmail.com

Paper History

Received: 19 - November - 2018
Received in revised form: 8 - December - 2018
Accepted: 30 - December - 2018

ABSTRACT

The development of oil and gas technology from shallow water to deep sea is a challenge for Indonesian Hydrodynamics Laboratory (IHL) to carry out the deep sea model testing by using experimental tank with limited depth. Truncation method should be used to solve this problem. Mooring systems that will be analyzed in this study are multi buoy-mooring with configuration variations: two and four buoy-mooring installed on the FPSO. A numerical analysis was performed for determining mooring system response to avoid time and cost consuming. Analysis was conducted using time domain analysis to obtain the configuration that produce minimum tension of mooring lines. Two buoy-mooring show a better result configuration than four buoy-mooring.

KEY WORDS: *Multi-Buoy ,Mooring, Tension*.

NOMENCLATURE

FPSO	Floating Production Storage and Offloading
LPG	Liquefied Petroleum Gas
RAO	Response Amplitude Operator (m/m or rad/rad)
ζ_{k0}	Amplitude of motion (m)
ζ_0	Wave amplitude (m)
k_w	Wave numbers
EA	Axial stiffness (kN)
D	Nominal diameter (m)
ε	Mean axial strain
L	Instantaneous length of segment (m)
L_0	Unstretched length of segment (m)
Te	Effective tension (kN)
v	Poisson ratio
P_0	External pressure (kN/m^2)
A_0	External cross section area (m^2)
P_i	Internal pressure (kN/m^2)
A_i	Internal cross section area (m^2)
E	Damping coefficient of the line (s)
dL/dt	Rate of increase of length

1.0 INTRODUCTION

FPSO is one type of floating structures. It is very dependent on the mooring system when operated in the water. Mooring system is used to restrict its movements that occurs when the floating structure suffered from environmental load, so that it can continue to operate safely. There are many kinds of mooring systems used for offshore platforms which are spread mooring, single buoy mooring, multi buoy mooring, and turret.

In their technical report, Odabasi, et al. review some LPG distribution company in the Gulf of Izmit, Marmara Sea, Turkey [1]. The company use various configuration of spread mooring. They usually prefer the cheapest solution in terms of initial investment cost. However, they must change the configuration numerous times because of some minor accidents and/or additional load capacity.

Mentes and Helvacioglu argued that the company will spend a lot of money and time to repair or rebuild the production facility, which in this case is the replacement of the mooring system configuration [2]. Therefore, the selection of the mooring system configuration is very important.

Analysis of the mooring system can be studied numerically and/or physically with laboratory experiment. The focus of this study was limited to numerical analysis, but further was followed by physical testing in IHL. This analysis was conducted to

ISOMAse
International Society of Ocean, Mechanical and Aerospace Scientists and Engineers
Journal of Subsea and Offshore
-Science and Engineering-
30th December 2018. Vol.16 No.1

December 30, 2018

determine the best configuration that will be used in physical testing, in order to save time and cost.

The purpose of this research series is to obtain a relationship which can represent real operational conditions by using model test. Considering the limitations of test facilities owned by IHL where the depth of the experimental tank for testing is only 2.5 m. FPSO operate at depths of 212 meters in this research. Model scale that should be used is 1:85 when considering the ocean depths, but the dimensions of the ship model will be very small. Unfortunately, it can not be done considering the capacity and dimension of the test equipment. In order to solve the problem, a truncation method should be applied to simulate amount of mooring line truncation before physical model test was performed.

Truncation method which applied in this research was purposed to reduce water depth and also the length of mooring lines as shown in Figure 1. The length reduction of mooring lines will certainly give an effect to the properties of its mooring line, so further analysis was required in order that truncation method can represent real conditions.

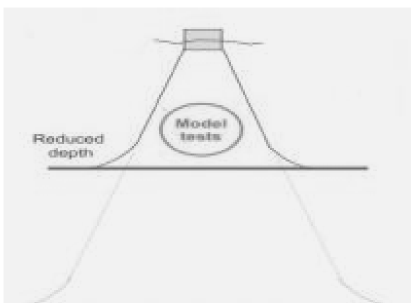

Figure 1: Truncation method [3].

Numerical analysis that will be discussed in this study is the usage of multi-buoy mooring as one of the mooring system that will be installed on the FPSO. Some variation in the configurations that will be applied are two and four buoy-mooring. The result is the tension produced by the mooring system due to the use of these configuration.

2.0 MODELING

The data used in this study are the structure of FPSO, mooring system, buoy, and environmental data. FPSO and buoy data used for modeling process that will be used for the structural analysis of motion behavior characteristic in free floating condition on regular wave. The analysis is often called hydrodynamic analysis where one of its output is RAO. Hydrodynamic analysis is obtained by using frequency domain analysis. RAO translational and rotational motion respectively can be seen in equation (1) and (2).

$$RAO = \frac{\zeta_{k0}}{\zeta_0}\ (m/m) \qquad (1)$$

$$RAO = \frac{\zeta_{k0}}{k_w \zeta_0} (rad/rad) \qquad (2)$$

Equation (1) is an equation to obtain RAO translational motion which is direct comparison between the amplitude of motion and the amplitude of wave. Equation (2) is an equation to obtain RAO rotational motion which is the ratio between the amplitude of motion and the slope of wave (the multiplication of wave number with amplitude of wave) [4].

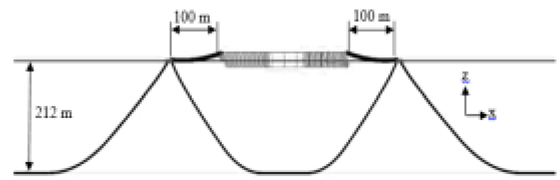

(a)

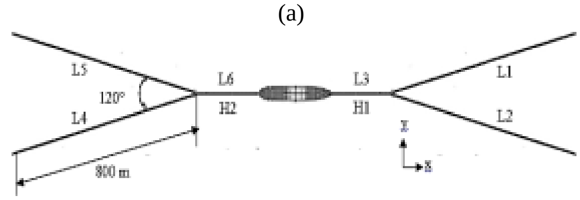

(b)

Figure 2: Two buoy-mooring configuration; (a) side view; (b) top view.

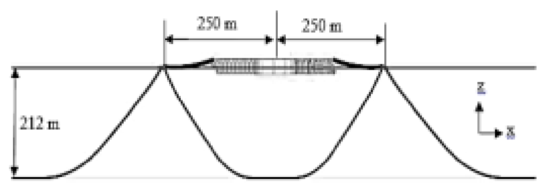

(a)

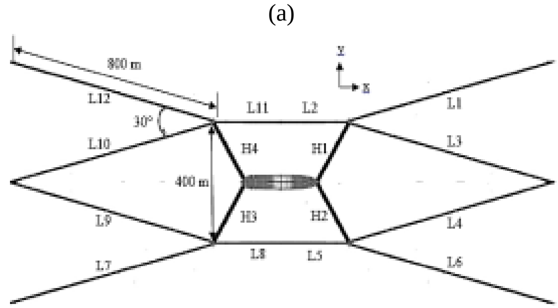

(b)

Figure 3: Four buoy-mooring configuration; (a) side view; (b) top view.

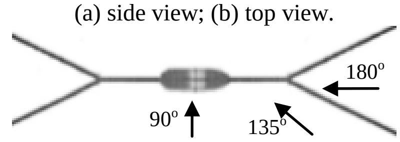

Figure 4: Layout of environmental loading.

The required data in the analysis of mooring system are RAO, added mass, damping, mean drift force, excitation force, and environmental data. All the data except the environmental data are obtained from hydrodynamic analysis. Analysis for the line tension is obtained by using time domain analysis. Environmental data used are wind, current and wave load. The equations used in the analysis of the time domain as follows:

JSOse | Received: 19 - November - 2018 | Accepted: 30 - December - 2018 | [(16) 1: 1-5]
Published by International Society of Ocean, Mechanical and Aerospace Scientists and Engineers, www.isomase.org., ISSN: 2442-6415

$$EA = 0.854x10^8D^2 \text{ for studless chain} \quad (3)$$

$$\varepsilon = \frac{L-L_0}{L_0} \quad (4)$$

$$T_e = EA.\varepsilon + (1-2v)(P_0A_0 - P_iA_i) + \frac{EA.e(dL/dt)}{L_0} \quad (5)$$

Modeling of the mooring system with two buoy-mooring configuration is illustrated in Figure 2, while four buoy-mooring configuration is illustrated in Figure 3. The mooring system is analyzed on three loading conditions that assumed wind, currents and waves to be collinear. The loading condition are head seas (heading of 180°), quarter seas (heading of 135°), and beam seas (heading of 90°). The loading condition can be seen in Figure 4.

3.0 RESULTS AND DISCUSSION

3.1 Tension of the Mooring Line

The dimensions of FPSO which is the length, width, height and draft of the ships are respectively 268.4, 41.6, 28 and 11.3 m. While the diameter, height and draft buoy respectively is 15, 4.5, and 2 m. Hawser, that has the properties of polypropylene, used to connect the ship and buoy. Each buoy was attached with three mooring lines. Mooring line configuration that was used consists of chain-rope-chain. Rope was used to reduce the weight of the mooring line at floating structures and to decrease mooring load with the elasticity of the material [5].

Table 1: The maximum tension in each mooring lines of two buoy-mooring configuration

Mooring line	At the end of buoy		At the end of anchor	
	Mean tension (ton)	Heading (°)	Mean tension (ton)	Heading (°)
L1	139.201	180	110.002	180
L2	557.508	90	528.496	90
L3	35.305	90	16.126	90
L4	537.195	90	508.212	90
L5	87.478	180	49.889	180
L6	99.229	180	78.852	180

In the heading of 180°, four buoy-mooring configuration produce lower tension in almost all mooring line, except for the mooring line L2 and L5 that has mean tension of 39.06 tons larger than two buoy-mooring configuration.

In the heading of 135°, two buoy-mooring configuration produce lower tension on the mooring line L1, L4 and L5 that has mean tension of 44.66, 217.57 and 12.82 tons larger than four buoy-mooring configuration.

In the heading of 90°, two buoy-mooring configuration produce lower tension in almost all mooring line, except the mooring line L4 and L5 that has mean tension of 477.42 and 7.85 tons larger than four buoy-mooring configuration.

Tension of the mooring line on both configuration can be seen in Table 1 and Table 2. While the difference value of tension between two and four buoy-mooring configuration can be seen in Table 3. Two buoy-mooring configuration produce lower line tension than four buoy-mooring configuration especially on a heading of 135° and 90°.

Table 2: The maximum tension in each mooring lines of four buoy-mooring configuration

Mooring line	At the end of buoy		At the end of anchor	
	Mean tension (ton)	Heading (°)	Mean tension (ton)	Heading (°)
L1	100.233	180	73.984	180
L2	95.276	90	76.005	90
L3	60.634	90	19.082	135
L4	60.274	90	20.496	135
L5	563.201	90	544.376	90
L6	584.594	90	555.527	90
L7	552.519	90	523.500	90
L8	556.744	90	537.915	90
L9	59.777	90	19.483	90
L10	57.387	90	11.939	90
L11	95.369	180	74.414	180
L12	52.065	180	10.928	180

Table 3: The difference value of tension between two buoy-mooring configuration and four buoy-mooring configuration

Heading (°)	Mooring line	Different values of tension (ton)	
		At the end of buoy	At the end of anchor
180	L1	-87.185	-94.767
	L2	-40.408	-36.835
	L3	39.057	36.800
	L4	-36.161	-39.921
	L5	-35.413	-38.960
	L6	-3.860	-4.438
135	L1	-44.660	-52.575
	L2	21.535	22.154
	L3	302.433	302.240
	L4	-217.568	-228.669
	L5	-12.821	-21.100
	L6	49.800	50.879
90	L1	1.123	-9.654
	L2	27.086	27.030
	L3	527.895	528.249
	L4	-477.418	-488.728
	L5	-7.845	-18.044
	L6	50.024	50.079

Note: (+) tension on two buoy-mooring configuration is smaller than four buoy-mooring configuration
(-) tension on two buoy-mooring configuration is larger than four buoy-mooring configuration

3.2 Time History of Line Tension

From the previous discussion, tension of the mooring line that occur in both configuration at each heading has been summarized. Wave profile for 3600 and 400 seconds simulation is shown in Figure 5. The results of time history that will be shown in this paper is the maximum response that occurs in the simulation that is at 2700-3100 seconds (400 seconds simulation). Figure 6 -

JSOse | Received: 19 - November - 2018 | Accepted: 30 - December - 2018 | [(16) 1: 1-5]
Published by International Society of Ocean, Mechanical and Aerospace Scientists and Engineers, www.isomase.org., ISSN: 2442-6415

ISOMAse
International Society of Ocean, Mechanical and Aerospace Scientists and Engineers

Journal of Subsea and Offshore
-Science and Engineering-
30th December 2018. Vol.16 No.1

Figure 8 were time history from each tension on numerical analysis. From the figure, it can be seen that the wave height is greatest in the 222 seconds.

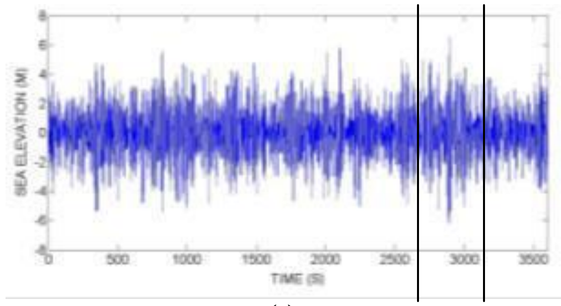

(a)

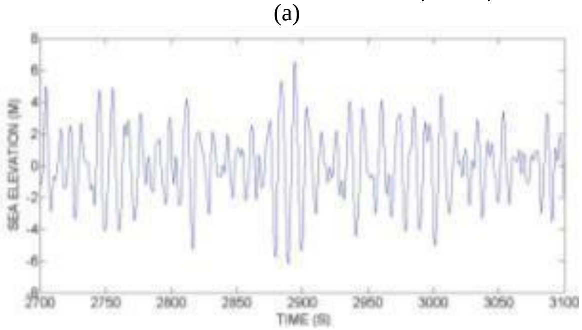

(b)

Figure 5: Sea surface elevation; (a) 3600 sec. simulation; (b) 400 sec. simulation.

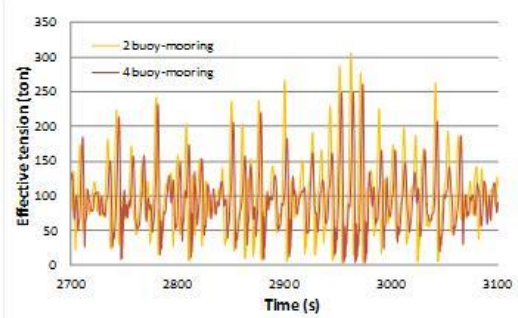

(a)

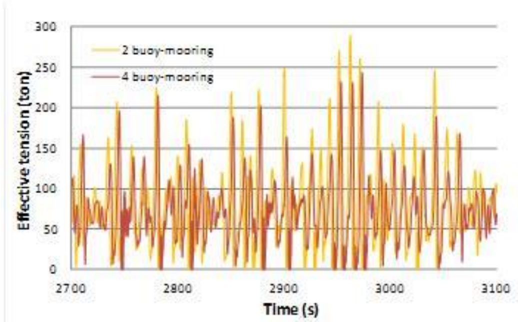

(b)

Figure 6: Tension of mooring line in the heading of 180°; (a) at the end of buoy; (b) at the end of anchor.

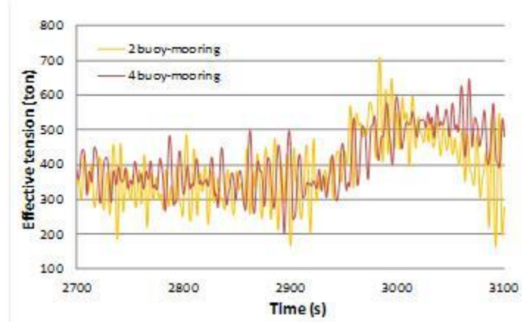

(a)

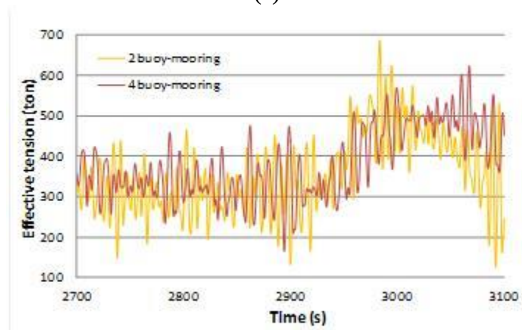

(b)

Figure 7: Tension of mooring line in the heading of 135°; (a) at the end of buoy; (b) at the end of anchor.

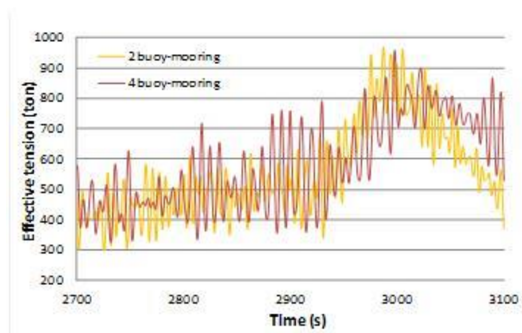

(a)

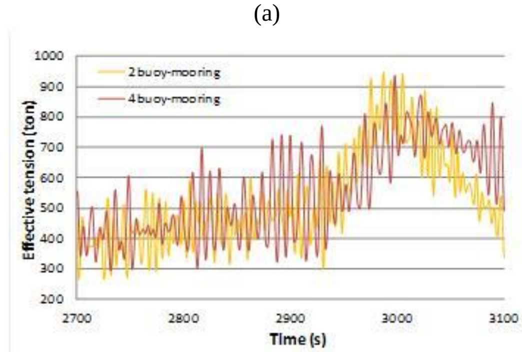

(b)

Figure 8: Tension of mooring line in the heading of 90°; (a) at the end of buoy; (b) at the end of anchor.

JSOse | Received: 19 - November - 2018 | Accepted: 30 - December - 2018 | [(16) 1: 1-5]
Published by International Society of Ocean, Mechanical and Aerospace Scientists and Engineers, www.isomase.org., ISSN: 2442-6415

Journal of Subsea and Offshore
-Science and Engineering-
30th December 2018. Vol.16 No.1

In the heading of 180°, almost in the whole simulation, four buoy-mooring configuration produce lower line tension than two buoy-mooring configuration, both in the tension that occur in the end of buoy and anchor.

In the heading of 135°, two buoy-mooring configuration produce lower line tension than four buoy-mooring configuration especially on simulation 0-30, 70-100, 130-160, 220-250, and 320-400 seconds, both in the tension that occur in the end of buoy and anchor.

In the heading of 90°, two buoy-mooring configuration produce lower line tension than four buoy-mooring configuration especially on simulation 100-240 dan 340-400 seconds, both tension that occur in the end of buoy and anchor.

4.0 CONCLUSION

Two buoy-mooring configuration produce lower tension on the moring line when compared with four buoy-mooring configuration at heading of 135^0 and 90^0. Whereas for heading of 180^0, four buoy-mooring configuration produce lower tension than two buoy-mooring configuration. By considering its result and operational costs, the configuration of two buoy-mooring was selected for physical model testing. There is an issues that has not been covered in this research. The issue is to check the natural frequency of the system (full mooring system installed on FPSO). Furthermore future work to be developed are variations in buoy diameter, mooring line diameter, mooring line material and number of segments in the mooring line (there are three or four types of wire/rope/chain on each line).

ACKNOWLEDGEMENTS
The authors are very grateful to Agency for The Assessment an Aplication of Technology (BPPT) for supporting this research.

REFERENCE

1. Odabasi, A. Y., Soylemez, M., Sarioz, K., Insel, M., Helvacioglu, I. H., and Unsan, Y. (2006). *Investigation on Yarimca Catenary Buoy Mooring (CBM) System*, Technical Report, ITU, NAOE Research and Application Group (Commercial in Confidence).
2. Mantes, A. and Helvacioglu, I. H. (2012). Fuzzy Decision Support System for Spread Mooring System Selection, *Expert System with Application Volume 39, pp: 3283-3297.*
3. Fylling,, I. J. and Stansberg, C. T. (2005). Model Testing of Deepwater Floating Production Systems: Strategy for Truncation of Moorings and Risers, *DOT 2005 Conference*, Brazil
4. Djatmiko, E. B. (2012). *Perilaku dan Operabilitas Bangunan Laut di Atas Gelombang Acak*: ITS Press, Surabaya.
5. Harnois, V., Smith, H. C. M., Benjamins, S., and Johanning, L. (2015). Assessment of Entanglement Risk to Marine Megafauna due to Offshore Renewable Energy Mooring Systems, *International Journal of Marine Energy Volume 11, pp: 27-49.*

JSOse | Received: 19 - November - 2018 | Accepted: 30 - December - 2018 | [(16) 1: 1-5]
Published by International Society of Ocean, Mechanical and Aerospace Scientists and Engineers, www.isomase.org., ISSN: 2442-6415